Optics Letters

Ultra-stable high average power femtosecond laser system tunable from 1.33 to 20 μm

Tobias Steinle,* Florian Mörz, Andy Steinmann, and Harald Giessen
4th Physics Institute and Research Center SCoPE, University of Stuttgart, Stuttgart, Germany
*Corresponding author: t.steinle@pi4.uni-stuttgart.de

Received 19 August 2016; revised 21 September 2016; accepted 26 September 2016; posted 27 September 2016 (Doc. ID 274061); published 17 October 2016

A highly stable 350 fs laser system with a gap-free tunability from 1.33 to 2.0 μm and 2.13 to 20 μm is demonstrated. Nanojoule-level pulse energy is achieved in the mid-infrared at a 43 MHz repetition rate. The system utilizes a post-amplified fiber-feedback optical parametric oscillator followed by difference frequency generation between the signal and idler. No locking or synchronization electronics are required to achieve outstanding free-running output power and spectral stability of the whole system. Ultra-low intensity noise, close to the pump laser's noise figure, enables shot-noise limited measurements.

OCIS codes: (190.4970) Parametric oscillators and amplifiers; (190.2620) Harmonic generation and mixing.

http://dx.doi.org/10.1364/OL.41.004863

A variety of applications, including remote sensing, multi-photon microscopy, frequency comb spectroscopy, and mid-infrared (MIR) imaging require flexible sources that provide tunable radiation in the 1–20 μm spectral range [1,2].

Quantum cascade lasers [3] have proven to provide MIR radiation with a compact setup, but with rather narrow spectral bandwidth and a limited tuning range [4,5]. Parallelization is required to cover the full MIR range. Optical parametric frequency conversion, in contrast, provides the opportunity to cover much broader spectral regions with a single system, since the accessible frequencies are only limited by the transparency of the nonlinear gain medium and the phase-matching condition. As optical parametric sources are often realized with femto- or picosecond pump lasers, they are particularly suited for time-resolved studies.

Such broadly tunable systems can be realized by difference frequency generation (DFG) of mode-locked Yb or Er lasers and a supercontinuum or redshifted solitonic radiation derived from the same oscillator [6–10]. Seidel *et al.* have recently demonstrated watt-level output at 8.5 μm using this concept [11].

Another approach is to use DFG between the signal and the idler of an optical parametric oscillator (OPO) or amplifier (OPA). Tuning ranges of 5–20 μm have been demonstrated with several tens of mW of output power in the femtosecond regime [12,13]. Further, DFG with the signal beams of a dual wavelength OPO has been demonstrated [14].

OPOs with MIR idler radiation can be realized [15,16], but 1 μm pumped systems are currently limited in tuning range due to the availability of nonlinear crystals.

Lastly, cascaded OPOs can be realized [17]. This results, however, in complex systems with limited tuning range and high demand on low loss optics. Moreover, a general issue when working with OPO-based systems is that applications suffer from their limited stability due to their sensitivity to ambient and pumping conditions. Active stabilization can mitigate these effects, but it will introduce artifacts at the control frequencies and increase complexity and cost.

In this Letter, we present a system which unites an ultra-broad tuning range (1.33–20 μm), a nJ level pulse energy in the MIR, and, importantly, both excellent long-term stability and low intensity noise, due to the use of a robust fiber-feedback optical parametric oscillator (ffOPO) [18–20].

The setup, as shown in Fig. 1, is based on a post-amplified ffOPO [21], which is directly pumped by a 1.03 μm, 7 W, 450 fs Yb:KGW oscillator at a 43 MHz repetition rate [22]. The system from [21] was slightly modified such that two 10 mm long fan-out periodically-poled lithium tantalate crystals (HC Photonics) with poling periods ranging from 24 to 34.5 μm are used for both the ffOPO and the OPA.

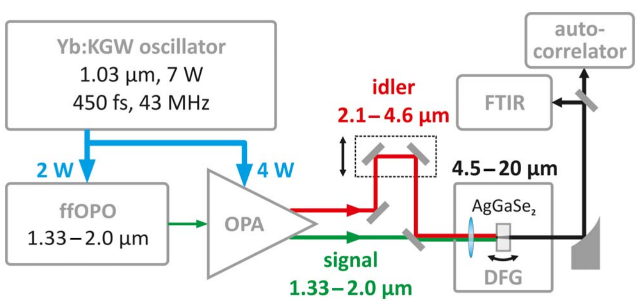

Fig. 1. Schematic setup. ffOPO, fiber-feedback optical parametric oscillator; OPA, optical parametric amplifier; DFG, difference frequency generation; FTIR, Fourier-transform infrared spectrometer.

This increased performance of the system in the 1.7–2.0 μm signal range is of key importance for the DFG between the signal and the idler. Here, we employ two $AgGaSe_2$ crystals to generate radiation from 4.5 to 20 μm.

The first crystal is cut for type I phase matching with $\theta = 53°$ and does not have an AR coating. The second crystal is cut for type II phase matching at $\theta = 51°$ and is AR coated for 1.7–2.6 μm at the input facet and for 9–16 μm at the output facet ($R < 6\%$). The details on phase matching, spatial and temporal walk-off, and the nonlinear coefficient can be found in [13]. Both crystals are 2 mm long. In both cases, the signal and idler beam were focused to a 35 μm waist using an uncoated CaF_2 lens with a 75 mm focal length. The 11–12 mrad spatial walk-off is not critical for both type I and type II phase matching and, thus, longer crystals could be employed for better power extraction. The characterization of the generated MIR pulses is carried out by a Fourier-transform infrared (FTIR) spectrometer and a home-built autocorrelator, while the power was measured using a thermal power meter. All power levels are reported as measured and are not corrected for atmospheric or filter losses, which are on the order of 10%–15% in the 1–10 μm range and higher above. The power meter was located closely to the $AgGaSe_2$ crystal to minimize atmospheric losses. In addition, the spectra were acquired with minimum propagation distance in air.

Figure 2 shows the tuning range of the entire system. Up to 2.8 W of power are obtained in the 1.33–2.0 μm signal range, while up to 0.81 W could be achieved in the idler range of 2.13–4.6 μm. The DFG tuning range is adjacent without a gap, starting at 4.5 μm, if the type I $AgGaSe_2$ crystal is used. Up to 94 mW (2.2 nJ) are generated at 5.5 μm, 28 mW at 10 μm, and 8 mW at 15 μm. 0.4 mW were generated at 20 μm. By employing the AR-coated type II crystal, higher MIR power levels of 40 mW at 10 μm, 16 mW at 15 μm, and 0.6 mW at 20 μm were achieved. Apart from the high average power extraction, the amplified ffOPO system features the advantage that the spectrum is tunable with sub-nm precision in the entire DFG range. Hence, the tuning range is completely gap-free except around the degeneracy of the ffOPO from 2.0 to 2.13 μm. Considering the missing AR coating of the type I crystal, we expect similar power levels for type I phase matching, if an AR-coated crystal would be used. This finding is in contrast to the fact that type II phase matching provides higher nonlinearity above a 8 μm DFG wavelength [13]. However, the crystal quality of our type I and type II crystals may differ and, thus, bias the comparison.

The pulse duration of the OPA signal was measured to be within the 250–400 fs range, with a typical time-bandwidth product (TBP) of 0.4–0.6 [21]. Utilizing a home-built interferometric autocorrelator based on two-photon absorption in an InGaAs diode, we confirmed the same pulse durations and TBP for the idler in the 2–4.5 μm spectral region. Here, we further investigate the pulse duration of the DFG pulses at 6.75 μm. Therefore, the autocorrelator was changed to a second-harmonic generation (SHG) configuration with another $AgGaSe_2$ crystal of 2 mm length for frequency doubling. An InAsSbP diode with a cutoff wavelength of 3.5 μm is employed to detect the autocorrelation trace. The wavelength of 6.75 μm is chosen to minimize atmospheric absorption due to the long propagation, while ensuring that the SHG is located sufficiently below the cutoff wavelength of the detector.

The free-space optical path length in air for the spectral measurement has been stretched to match the path length in the autocorrelator. Figure 3 shows both the optical spectrum (a) and the corresponding autocorrelation (b), indicating a pulse duration of 383 fs for a Gaussian pulse shape. With a spectral bandwidth of 209 nm, obtained by a Gaussian fit, the resulting time-bandwidth product is 0.53, which is an excellent value compared to previous reports [13], despite the fact that the spectrum is distorted by some atmospheric absorption. We attribute this to the high-quality pump pulses from the OPA on the one hand and the relatively short nonlinear crystal on the other hand, which minimizes temporal distortion due to the group velocity mismatch.

In contrast to their free-space counterparts, ffOPOs are very robust to changes in ambient or pumping conditions. Thus, stable performance is warranted in the entire tuning range. We demonstrate this by recording the free-running power

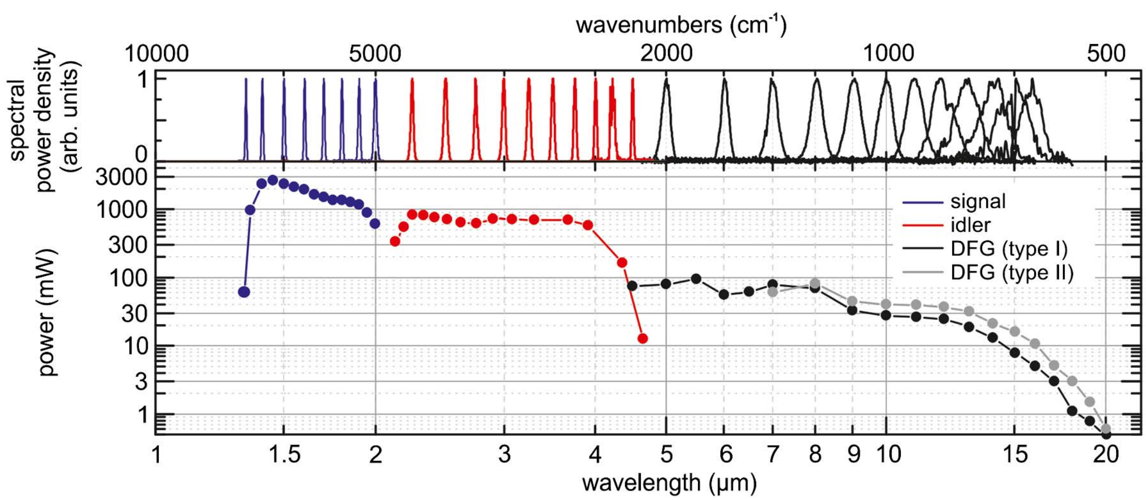

Fig. 2. Spectra and average power of the entire system including watt-level output in the signal (blue) and idler (red) range and up to 94 mW average power in the DFG range using type I (black) and type II (gray) phase matching. The mid-infrared spectra were recorded with a resolution of 4 cm^{-1}, using the type I phase-matched crystal.

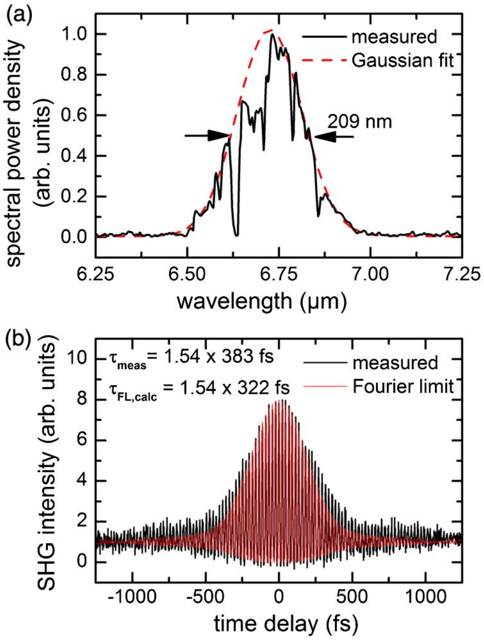

Fig. 3. Spectrum with 2 cm^{-1} resolution at (a) at 6.75 µm center wavelength and (b) corresponding interferometric SHG autocorrelation. The pulse durations are calculated from the measured autocorrelation width assuming a Gaussian pulse shape.

and spectral stability of the DFG beam at 8 µm. Figure 4 shows that the rms power fluctuation over 4 h was 0.38%, with a maximum peak-to-peak difference of 1.5%, which is on the level of the performance of mode-locked oscillators. The spectral drift is negligible, even over longer periods without any active stabilization, as illustrated in Fig. 4(b). This is a result of the combination of the ffOPO and the OPA, which decouples the control parameters, such as wavelength and pulse duration (ffOPO) and final output power (OPA). In a conventional OPO, these parameters would be closely coupled, and sophisticated dispersion management and piezo-controlled cavity length would be required. Further, the atmospheric absorptions that are present in both the OPA signal and the idler range did not lead to drifts in the DFG power or the center wavelength over the tuning range, which underlines the robustness of the concept.

The relative intensity noise (RIN) was measured with a home-built low-noise, 20 MHz low-pass-filtered, transimpedance amplifier detector circuit using an InGaAs detector (Hamamatsu G12182-003K). The detector's noise figure, which was measured with blocked light, is below the shot noise for 1.5 mA photo current in the 10 kHz–20 MHz range, as depicted in Fig. 5.

The measured RIN of both the ffOPO and the OPA running at maximum output power is found to be close to the RIN of the Yb:KGW pump laser. Both the Yb:KGW oscillator and the OPA possess an excellent noise figure with shot-noise-limited performance (−154 dBc/Hz) from 400 kHz onward. All measurements show some excess noise at 65 kHz, which arises from the relaxation oscillations in the Yb gain medium of the pump laser. The overall noise level is very low due to the solid-state pump laser.

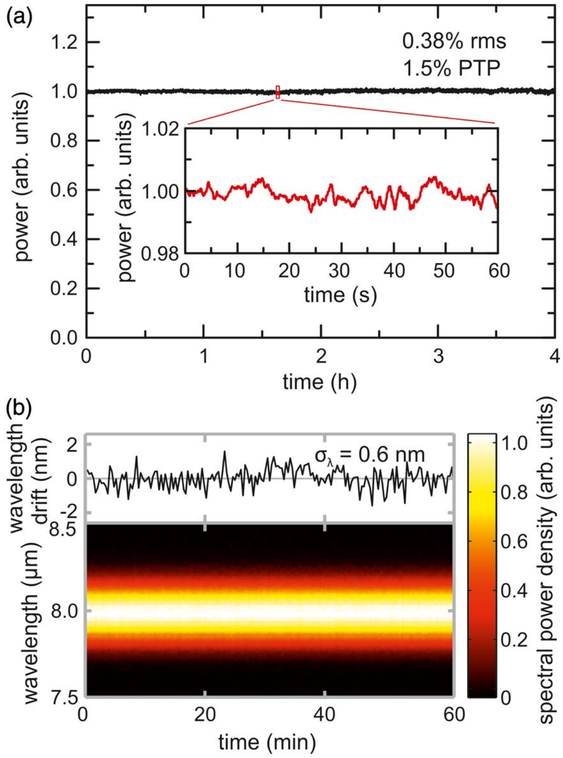

Fig. 4. Power stability of the DFG output at 8 µm over (a) 4 h and 60 s (inset), sampled at 10 Hz, as well as the spectral drift stability over 60 min. Three spectra per minute were used for (b). The resolution was 2 cm^{-1}. The upper plot shows the center wavelength drift obtained from a Gaussian fit.

While at low-signal wavelengths, the OPA exhibits slightly higher noise compared to the pump laser; we found a better noise figure compared to the pump laser when the OPA was operated at 1800 nm. We attribute this behavior to the different single-pass gain of the parametric frequency conversion in the ffOPO. As a result of the extreme single-pass gain of up to 60 in the 1500 nm region [21], the ffOPO is operated at a very low feedback (5%–10%). At 1800 nm, in contrast, a relatively high feedback (∼50%) is required and, hence, the ffOPO is less

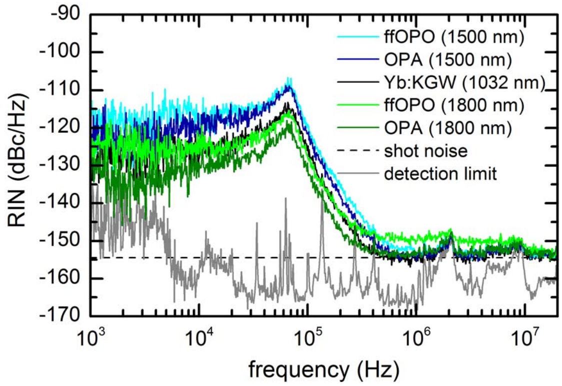

Fig. 5. Relative intensity noise comparison of the Yb:KGW oscillator (black) and the signal of the ffOPO at 1500 nm (blue) and the OPA (dark blue), as well as the signal at 1800 nm (green and dark green). All measurements were taken with 1.5 mA photo current.

susceptible to fluctuations of the pump laser, but also less output power can be extracted. Due to the lack of detectors beyond 2 μm, it is not feasible to measure the noise figure of the idler and the DFG at the extremely low noise level of our system. Previously, it was demonstrated that signal and idler in OPAs exhibit similar noise figures [2] and, thus, no significant excess noise would be expected for any of the beams.

In conclusion, we have demonstrated a broadly tunable (1.33–20 μm) 350 fs laser system with nearly transform-limited pulses and an excellent noise figure, both in the RF domain and over several hours in free-running operation.

Its MIR output is ideally suited for frequency comb spectroscopy and mid-infrared imaging using focal plane arrays, as well as for remote sensing in the atmospheric windows. The ultra-low noise figure is advantageous for sensitive microscopic applications, such as vibrational sum-frequency spectroscopy or scanning near-field optical microscopy.

Novel nonlinear crystals [16,23] could be used for more efficient DFG to extract higher average power.

Funding. European Research Council (ERC) (COMPLEXPLAS); Bundesministerium für Bildung und Forschung (BMBF); Carl-Zeiss-Stiftung; Deutsche Forschungsgemeinschaft (DFG); Baden-Württemberg Stiftung (PROTEINSENS, Spitzenforschung II).

REFERENCES

1. K. Haase, N. Kröger-Lui, A. Pucci, A. Schönhals, and W. Petrich, J. Biophotonics **9**, 61 (2016).
2. F. C. Cruz, D. L. Maser, T. Johnson, G. Ycas, A. Klose, F. R. Giorgetta, I. Coddington, and S. A. Diddams, Opt. Express **23**, 26814 (2015).
3. J. Faist, F. Capasso, D. L. Sivco, C. Sirtori, A. L. Hutchinson, and A. Y. Cho, Science **264**, 553 (1994).
4. R. Maulini, M. Beck, J. Faist, and E. Gini, Appl. Phys. Lett. **84**, 1659 (2004).
5. A. Hugi, R. Terazzi, Y. Bonetti, A. Wittmann, M. Fischer, M. Beck, J. Faist, and E. Gini, Appl. Phys. Lett. **95**, 061103 (2009).
6. C. Erny, K. Moutzouris, J. Biegert, D. Kühlke, F. Adler, A. Leitenstorfer, and U. Keller, Opt. Lett. **32**, 1138 (2007).
7. A. Ruehl, A. Gambetta, I. Hartl, M. E. Fermann, K. S. E. Eikema, and M. Marangoni, Opt. Lett. **37**, 2232 (2012).
8. J. Krauth, A. Steinmann, R. Hegenbarth, M. Conforti, and H. Giessen, Opt. Express **21**, 11516 (2013).
9. T. Steinle, A. Steinmann, R. Hegenbarth, and H. Giessen, Opt. Express **22**, 9567 (2014).
10. I. Pupeza, D. Sánchez, J. Zhang, N. Lilienfein, M. Seidel, N. Karpowicz, T. Paasch-Colberg, I. Znakovskaya, M. Pescher, W. Schweinberger, V. Pervak, E. Fill, O. Pronin, Z. Wie, F. Krausz, A. Apolonski, and J. Biegert, Nat. Photonics **9**, 721 (2015).
11. M. Seidel, G. Arisholm, O. Pronin, and F. Krausz, in *Conference on Lasers and Electro-Optics*, OSA Technical Digest (Optical Society of America, 2016), paper STu3I.6.
12. M. Beutler, I. Rimke, E. Büttner, V. Petrov, and L. Isaenko, Opt. Lett. **39**, 4353 (2014).
13. M. Beutler, I. Rimke, E. Büttner, P. Farinello, A. Agnesi, V. Badikov, D. Badikov, and V. Petrov, Opt. Express **23**, 2730 (2015).
14. R. Hegenbarth, A. Steinmann, S. Sarkisov, and H. Giessen, Opt. Lett. **37**, 3513 (2012).
15. S. Chaitanya Kumar, J. Krauth, A. Steinmann, K. T. Zawilski, P. G. Schunemann, H. Giessen, and M. Ebrahim-Zadeh, Opt. Lett. **40**, 1398 (2015).
16. L. Maidment, P. G. Schunemann, and D. T. Reid, Opt. Lett. **41**, 4261 (2016).
17. S. Marzenell, R. Beigang, and R. Wallenstein, Appl. Phys. B **69**, 423 (1999).
18. T. Südmeyer, J. Aus der Au, R. Paschotta, U. Keller, P. G. R. Smith, G. W. Ross, and D. C. Hanna, Opt. Lett. **26**, 304 (2001).
19. K. A. Ingold, A. Marandi, M. J. F. Digonnet, and R. L. Byer, Opt. Lett. **40**, 4368 (2015).
20. T. Steinle, F. Neubrech, A. Steinmann, X. Yin, and H. Giessen, Opt. Express **23**, 11105 (2015).
21. F. Mörz, T. Steinle, A. Steinmann, and H. Giessen, Opt. Express **23**, 23960 (2015).
22. A. Steinmann, B. Metzger, R. Hegenbarth, and H. Giessen, in *Conference on Lasers and Electro-Optics (CLEO): Laser Applications to Photonic Applications*, OSA Technical Digest (Optical Society of America, 2011), paper CThAA5.
23. M. Beutler, I. Rimke, E. Büttner, V. Badikov, and V. Petrov, *High-Brightness Sources and Light-Driven Interactions*, OSA Technical Digest (online) (Optical Society of America, 2016), paper MT2C.3.